Fibers Spun from Blends of Different Molecular Weights of Polypropylene

S. J. MAHAJAN, K. BHAUMIK, and B. L. DEOPURA

Textile Technology Department, Indian Institute of Technology, New Delhi-110016, India

SYNOPSIS

Fibers spun from blends of small percentage of plastic grade polypropylene (HMPP) with fiber grade polypropylene (PP) are studied for drawing behavior. A factorial design of experiment is used for a two-stage drawing process with variables, such as percent of HMPP component, first stage draw ratio and temperature, and second stage temperature. Optimization is carried out for breaking stress and modulus of drawn filaments. Breaking stress of up to 0.74 GPa and initial modulus of 7.34 GPa is possible by such an optimization process. These properties are observed for 6% HMPP blend composition. Heat setting of drawn filaments show little changes up to 140°C heat-setting temperature. Large scale structural changes with rapid drop in mechanical properties is observed for 150–160°C heat-set samples.

INTRODUCTION

Addition of a small percentage of high molecular weight polymer in fiber-grade polymer may be used to advantage in improving properties of the filaments. Studies of Hinrichsen and Green[1] on nylon indicate that blending of a small percentage of high molecular weight material does not affect the melt viscosity of the parent component to any large extent. Results on polypropylene (PP) by Deopura and Kadam[2] supports this fact. Thus, properties of drawn polypropylene filaments can be significantly improved by blending with a small percentage of high molecular weight polypropylene (HMPP). These improvements are related to (a) a distorted spherulitic structure at the spinning stage, (b) increased amorphous orientation, (c) long chain molecules acting as tie chains, and (d) a possible reduction in crystal size.[2]

The drawing process of polypropylene and blends is greatly affected by the percentage of second component and drawing parameters. Bet et al.[3] carried out studies on drawn fibers, prepared by a two-stage drawing process from polypropylene and blends of polypropylene with 3% of HMPP. A factorial design of the experiment was used to optimize drawing variables, i.e., the first zone draw ratio, temperature, and the second zone temperature. A combination of 5.2 ×, 50°C, and 120°C for the three variables, respectively, for PP, gave an optimum tenacity of 8.8 gpd and an initial modulus of 94 gpd. The 3% HMPP blend sample gave a tenacity of 9.0 gpd and a modulus of 105 gpd at the variables, i.e., 4.9 ×, 40°C, and 127°C, respectively.

The present investigation deals with optimization of drawing variables for breaking stress and modulus of drawn filaments and studying the effect of heat-setting temperatures on mechanical and structural properties of filaments from PP and blends of PP with HMPP.

EXPERIMENTAL

Materials

Characteristics of two kinds of polypropylene chips used for this study are given in Table I.

Sample Preparation

A laboratory model Fuji melt spinning tester (Type C) was used for production of filaments. During the spinning process, spun filaments after emerging

Journal of Applied Polymer Science, Vol. 43, 49–56 (1991)
 CCC 0021-8995/91/010049-08$04.00

Table I Material Characteristics

Sample	Manufacturing Code	MFI	$\overline{M_v}$
PP	Pro-fax NESTE VC-19	14.5	104,000
HMPP	IPCL S-1730	1.7	322,000

from the spinnerette were quenched in a water bath maintained at 8°C. The distance between spinnerette and water bath was 350 mm. For all samples, a take-up speed of 80 m min^{-1} and a spin draw ratio of 72 was maintained throughout the spinning process. As-spun filament birefringence and density crystallinity values were in the range of $12–14 \times 10^{-3}$ and 52–55%, respectively. A two-stage drawing was carried out for these filaments, using a factorial design of the experiments. The variables for factorial design are (a) first zone draw ratio λ_1, (b) first zone temperature T_1, (c) second zone temperature T_2, and (d) HMPP composition. The samples are drawn to a maximum draw ratio in the second zone. A total of 31 drawing experiments are carried out. Details of factorial design and drawing conditions are given in the Appendix.

Heat setting of selected samples was done for PP, 6 and 12% HMPP drawn samples. The drawing conditions for the selected samples were optimum conditions as obtained from optimization technique. These conditions refer to λ as 2.5 $\times$, T_1 as 55°C, and T_2 as 130°C. Heat setting of these filaments was carried out in a silicon oil bath at temperatures of 100, 120, 140, 150, and 160°C for 10 min in a taut condition. After heat setting, samples were slowly cooled in a taut condition to room temperature and washed with carbon tetrachloride.

Characterization of Drawn and Heat-Set Filaments

Mechanical properties of filaments were measured on an Instron tensile tester (Model 4202) at a 100% strain rate with a gauge length of 50 mm. The initial modulus was calculated from the initial slope of the stress–strain curve.

Dynamic Mechanical Properties

The dynamic mechanical properties of drawn and heat-set filaments were measured in the tensile mode, using a Rheovibron (Model DVV II-EP). Measurements were carried out at 3.5 Hz as a function of temperature from −50 to +150°C, with a heating rate of 3°C min^{-1}.

Density

Density of samples were measured on a Davenport density gradient column maintained at 23 ± 2°C, using a mixture of isoproponal and diethylene glycol.

Crystallinity

Volume fraction crystallinity (X_v) from density was determined using crystalline and amorphous density as 0.946 and 0.853 g cm^{-3},[4] respectively. X-ray crystallinity (X_c) was determined from WAXD, applying the Farrow–Preston[5] method.

Crystal Size

Crystal size was estimated from WAXD patterns using Scherrer's equation:

$$D_{hkl} = \frac{0.89\bar{\lambda}}{\beta \cos \theta_{hkl}} \quad (1)$$

where D_{hkl} is the average dimension of the crystallites normal to the diffraction planes (hkl), $\bar{\lambda}$ is the wavelength (1.542 Å), β is the integral breadth of the reflection in radians, and θ is Bragg's angle. Corrections due to instrumental broadening were calculated and found to be negligible.

Birefringence, Crystalline Orientation Factor and Amorphous Orientation Factor

Birefringence Δn of the samples was measured on a Leitz polarizing microscope, Model Laborlux 12 POL with a Leitz Wetzler tilting-plate-type compensator. The accuracy for measurement of Δn is ± 0.002.

The crystalline orientation factor, f_c, was estimated from the azimuthal intensity distributions of the (110) and (040) reflections using Wilchinsky's[6] method. The amorphous orientation factor f_a was calculated using the Stein–Norris[7,8] method.

Coupling Parameter and Fraction of Tie Molecules

The modulus of drawn sample E is calculated on the basis of the Takayanagi[9,10] model using the following equation:

$$E = (1 - \lambda)E_c + \left[\frac{(1 - \Phi)}{E_c} + \frac{\Phi}{E_a}\right]^{-1} \quad (2)$$

where E_c is the crystal modulus along the molecular axis, E_a is the modulus of the amorphous phase except for tie molecules, and Φ and λ are the measures

of fraction of series and parallel coupling of the amorphous phase. λ is equal to the volume fraction of the amorphous region, V_a. If $\Phi = V_a/\lambda$ is substituted in

$$(1 - \lambda) = \frac{V_a E(E_c - E_a) - E_a(E_c - E)}{V_a E_c(E_c - E_a) - E_a(E_c - E)} \quad (3)$$

The fraction of tie molecules, $(1 - \lambda)$, was evaluated from eq. (3). The effective crystalline and amorphous modulii of PP for calculations were taken as 34 and 10^{-2} GPa, respectively.[10]

RESULTS AND DISCUSSION

Mechanical Properties of As-Spun Filaments

Yield stress (σ_y) and maximum draw ratio (MDR) of as-spun filaments are plotted as a function of HMPP blend composition in Figure 1. It is observed that both σ_y and MDR show increase with HMPP blend composition up to 6%. A further increase in HMPP composition show reduction in both σ_y and MDR.

Drawing behavior is critically dependent on the properties of as-spun filaments. In the present investigation, filaments are quenched at 8°C to generate essentially a dominant pseudohexagonal structure.[11] Addition of HMPP in PP generates a bimodal crystal texture as a result of the epitaxial attachment of the chains to growing lamellae crystallites.[12] These above factors help improve drawability of the blended as-spun filaments.[13] Macroscopically there have been several attempts to correlate σ_y and MDR with mean spherulitic diameter.

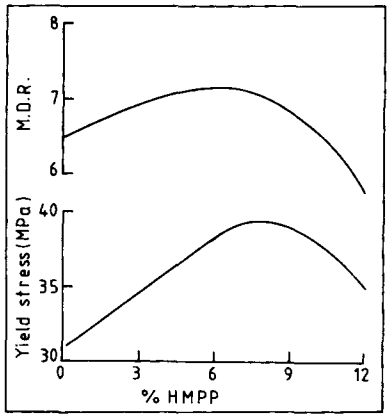

Figure 1 Yield stress and MDR of as-spun PP and PP/HMPP blend filaments.

A study[2] of the PP/HMPP blend system has shown that spherulite size decreases with the addition of HMPP up to 5% composition. It is also observed by other authors[14,15] that the very fine spherulitic microstructure produced by adding nucleating agents or reducing crystallization temperature results in improved ductility and increased yield stress. It is suggested that the possibility of the presence of highly interconnected interspherulitic matter at low HMPP compositions resists the initial deformation and thus increases the σ_y to some extent. During plastic deformation these interconnected spherulitic chains also act as a catalyst to effectively break up the spherulites through formation of several micronecks in the primary neck region.

At still higher HMPP compositions, very high molecular weight PP molecules are preferentially rejected from the spherulites (crystallization process) and segregate at the interspherulitic region. During the deformation process, this coarse spherulitic macrostructure and interspherulitic foreign matter layer lead to reduced σ_y. Further, such a structure gives fracture site at spherulite boundaries, reducing MDR.

Optimization of Drawing Variables

A factorial design of experiments has been carried out using drawing parameters as λ_1, T_1, T_2, and percent HMPP. Factorial design and experimental data for 31 samples are given in the Appendix. This analysis is used for optimization of strength and initial modulus. An effort to fit the strength values in a second-order polynomial equation in the analysis of factorial design was not successful. It was realized that the value of 0.85 GPa for sample 8 could not be fit in with a second-order polynomial. Therefore, it was decided to assume a breaking stress value of sample 8 as 0.76 GPa instead of 0.85 GPa. A good fit was obtained. F (model), the coefficient of determination (R^2), and the standard error of estimate are shown in Table IV (Appendix) with an F value of 0.83. A very large value of breaking stress for sample 8 (0.85 GPa) may be associated with synergistic effects. The following analysis is based on the assumed value of sample 8.

Figure 2(A) shows the dependence of breaking stress and modulus for the simultaneous variation of first zone temperature T_1 and HMPP composition for drawn filaments. It is observed that strength and modulus increases with increase in T_1 up to 55°C. Beyond this temperature, mechanical properties show a decreasing trend. The above effect can be explained in the following manner.

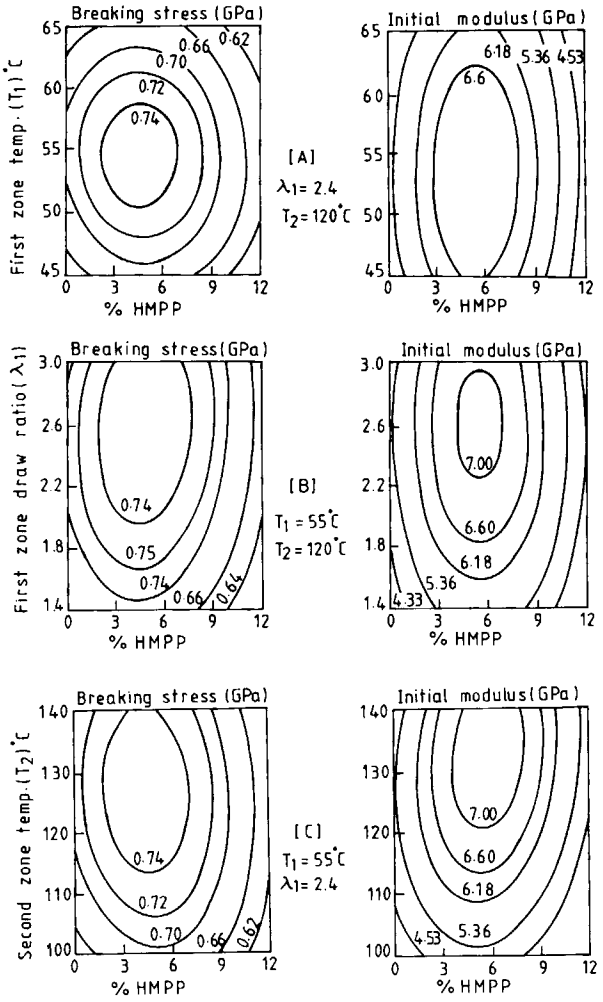

Figure 2 Breaking stress and initial modulus of fully drawn PP and PP/HMPP blend filaments: (A) effect of first zone temperature (T_1); (B) effect of first zone draw ratio (λ_1); (C) effect of second zone temperature (T_2).

For the filaments drawn at lower T_1, the motion available for the molecules to rearrange themselves in the orientation direction is much less. At this stage, the flaw mechanism (stress concentration) will predominate; the sample will only show extension due to crack formation and the strength of the filaments will be low. At higher T_1, the molecules have enough mobility for rearrangement of the internal structure to relieve the stress. At this stage, the spherulitic structure is slowly destroyed, and a microfibrillar structure develops. At still higher T_1, relaxation takes over the orientation process. The optimum T_1 is around 55°C.

Figure 2(B) shows the effect of first zone draw ratio λ_1 and HMPP composition on mechanical properties of drawn filaments. The initial increase in mechanical properties up to 2.5 × draw ratio is related to straightening of the interlocked chain molecules and uniform conversion of spherulitic to fibrillar structure, being the NDR of the sample. Deformation beyond NDR in the first zone induces a build in stresses in the structure as a result of higher orientation, and this leads to a relaxation process in the second zone drawing and lower strength and modulus values. Thus the optimum conditions of the first zone drawing are λ_1 as 2.5 × and T_1 as 55°C. This shows that the optimum λ_1 is close to NDR at given T_1.

The effect of the second zone temperature T_2 and HMPP composition on mechanical properties is shown in Figure 2(C). It is observed that the optimum value of T_2 for getting maximum strength and modulus is in the range of 120–130°C, and is related to enhanced mobility for the orientation process with a restricted relaxation process. Further investigations are in progress to ascertain synergistic improvements in strength for sample 8 prepared from 3% HMPP composition with T_1 as 55°C, λ_1 as 2.6×, and T_2 as 130°C.

Structural Characterization of Heat-Set Filaments

Crystallinity and Crystal Size

The dependence of crystallinity and crystal size on heat-setting temperature is shown in Figure 3. The degree of crystallinity measured by the X-ray and density method shows an increase with heat-setting temperature. The rapid increase in density and X-ray crystallinity with increasing temperature refers

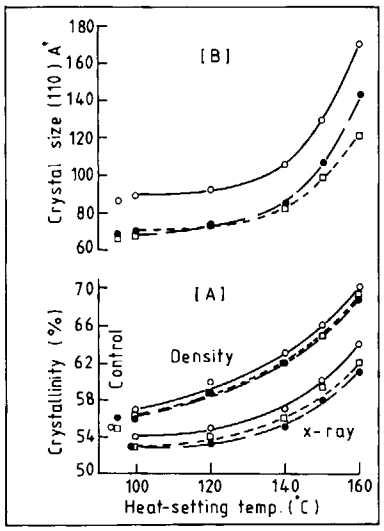

Figure 3 Crystallinity and crystal size (110) as a function heat-setting temperature for: (–○–) PP; (– –□– –) 6% HMPP; (–●–) 12% HMPP.

to a separation of crystalline and amorphous regions as distinct phases. No significant difference in crystallinity is observed for different HMPP blend samples. Increase in crystal size with temperature of thermal treatment for all set of samples is in general agreement with published work.[16-18] This process is attributed to a crystal perfection phenomenon at boundary layers of crystalline and amorphous phases and greater electron density differences between crystalline and amorphous regions.

It is most interesting to note that 6% HMPP sample has smaller crystal size compared to PP and 12% HMPP samples. This observation can support the possibility of a larger number of intercrystalline TTM present in the structure.

Birefringence, Crystalline and Amorphous Orientation

Birefringence Δn, crystalline orientation f_c, and amorphous orientation f_a as a function of heat-setting temperature is shown in Figure 4. As shown in Figure 4, f_a decreases with temperature. The rapid decrease in f_a beyond 120°C is obviously because of gross relaxation of the molecules in the amorphous region during reorganization of the structure at high temperatures. This process increases f_c to some extent. It is also observed that the addition of a small percentage of HMPP in PP considerably changes the process of molecular relaxation in amorphous regions, which can be seen from the trend observed for these samples. The ability of these samples to retain f_a is relatively higher compared to PP at high heat-setting temperatures and is related to the presence of higher TTM molecules present in the structure.

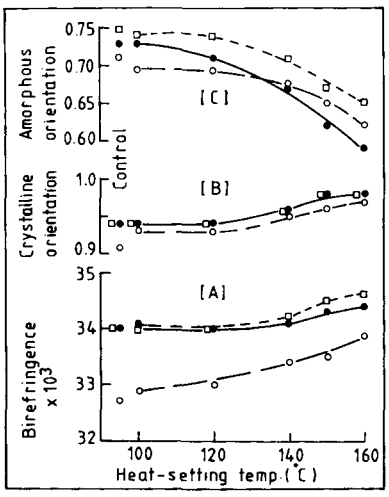

Figure 4 Birefringence, crystalline orientation function (f_c) and amorphous orientation function (f_a) as a function of heat-setting temperature for: (- ● -) PP; (- - □ - -) 6% HMPP; (- ○ -) 12% HMPP.

Mechanical Properties of Heat-Set Filaments

The initial modulus, breaking stress, and breaking strain are shown as a function of heat-setting temperature in Figure 5. Further, the initial modulus has been analyzed in terms of the Takayanagi unit cube model, assuming series and parallel couplings.[10] Series coupling is given by λ and parallel coupling is by Φ. The values of the coupling parameter ratio Φ/λ and fraction TTM $(1 - \lambda)$ are also shown in Figure 3. With increasing heat-setting temperature, it is observed that there is continuous increase in series coupling, whereas parallel coupling goes on decreasing. The fraction TTM decreases much more rapidly beyond 140°C. These observations are consistent with an increase in phase segregation of crystalline and amorphous regions and disorientation of the amorphous region. This is further supported by amorphous orientation function results given above.

Interesting observations are given by maxima in strength at 140°C and a large increase in strength for 6% HMPP sample at this temperature. This high strength of the HMPP sample is related to high f_c and with a marginal decrease in f_a. It is well known that, during heat setting of PP, crystalline orientation increases and this accounts for the large strength at a heat-setting temperature of 140°C. For 6% HMPP samples a large increase in strength is related to relatively high TTM as indicated by the analysis of the modulus by the unit cube model. The increase in breaking strain with increasing heat-setting temperature is related to decreasing f_a values.

Dynamic Mechanical Properties of Drawn and Heat-Set Filaments

Figure 6 shows dynamic mechanical behavior of drawn and 140°C taut annealed PP and 6% HMPP samples. It is observed that the drawn sample has a well-resolved tan δ peak at 0°C; however, the peak height decreases on taut annealing. This is related to increase in crystalline orientation during annealing. The E' values for 6% HMPP samples are slightly higher than PP samples and support the static mechanical results. The broad tan δ peak around 85°C is related to defect migration in the crystals, as well as in the interphase boundary between crystalline and amorphous regions.[19]

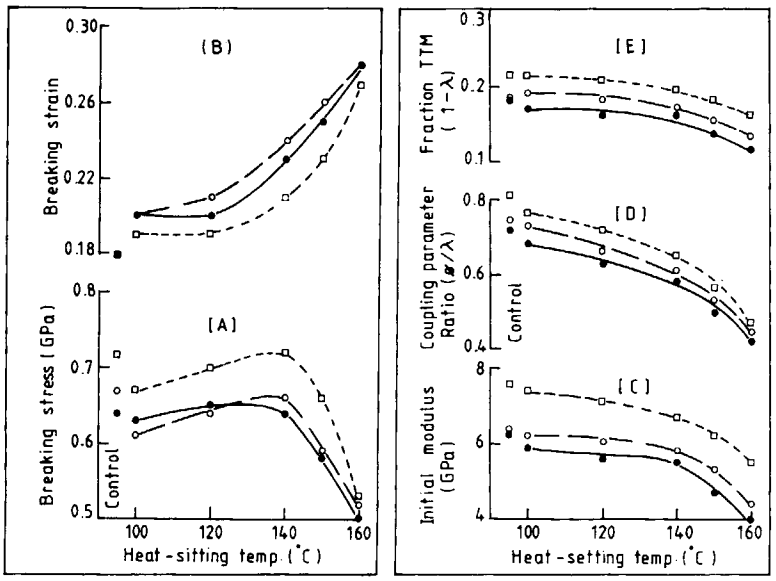

Figure 5 Effect of heat-setting temperature on: (A) breaking stress; (B) breaking strain; (C) initial modulus; (D) coupling parameter ratio (ϕ/λ); (E) fraction TTM ($1 - \lambda$): (- ● -) PP; (- - □ - -) 6% HMPP; (- ○ -) 12% HMPP.

CONCLUSIONS

Optimum breaking stress and modulus of the drawn samples is achieved at about 6% HMPP blend composition, when T_1 is 55°C, λ_1 is 2.5 ×, and T_2 of 120 and 127°C, respectively.

The overall increased values of strength and modulus for the 6% HMPP sample are a result of long molecular chains of the HMPP fraction acting as interconnecting links between crystalline regions. On the other hand, inferior strength and modulus at a relatively high percentage of the second component are related to phase segregation of long chain molecules of HMPP fractions.

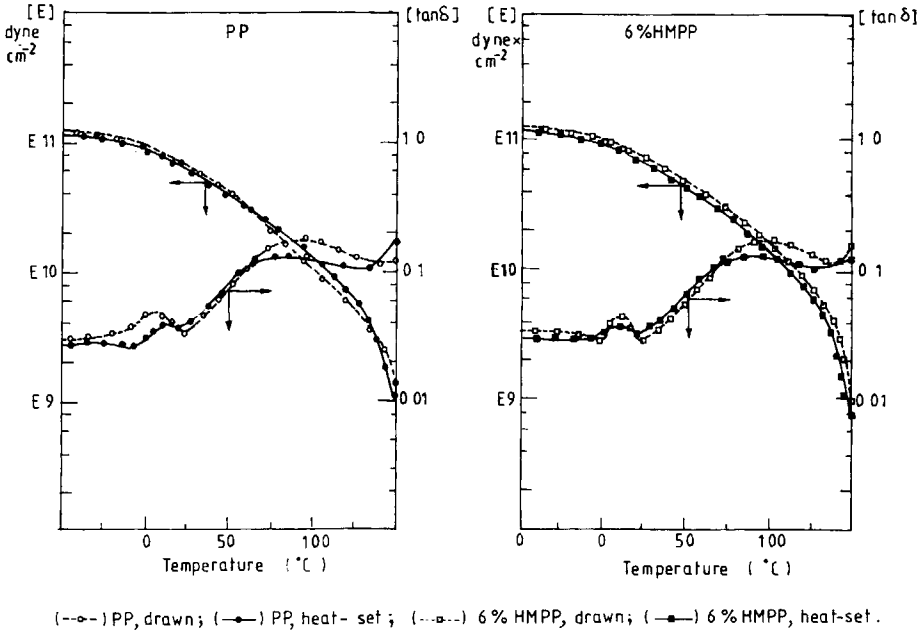

Figure 6 Dynamic mechanical properties of drawn and heat-set filaments: (- ● -) PP, drawn; (- - ○ - -) PP, heat-set; (- ■ -) 6% HMPP, drawn; (- - □ - -) 6% HMPP, heat-set.

Table II Process Variables and Unit Values

Variable	Unit Value				
	−2	−1	0	1	2
X_1 First zone temp. (T_1 °C)	45	50	55	60	65
X_2 First zone draw ratio (λ_1)	1.4	1.8	2.2	2.6	3.0
X_3 Second zone temp. (T_2 °C)	100	110	120	130	140
X_4 HMPP blend composition (B%)	0	3	6	9	12

During heat setting, taut tie molecules rearranges themselves in a state of lowest potential energy. This process results in a detectable change in amorphous orientation and crystallinity and consequently mechanical properties of the filaments. Optimum properties for heat-set samples are obtained for the 6% HMPP sample.

APPENDIX: MATHEMATICAL MODEL FOR OPTIMIZATION TECHNIQUE

Three drawing variables, namely, first zone temperature (T_1), first zone draw ratio (λ_1), second zone temperature (T_2), and one material variable, i.e., HMPP blend composition (%) along with five levels,

Table III Experimental Points with Mechanical Properties and Birefringence of Drawn Samples

Expt	T_1, X_1	λ_1, X_2	T_2, X_3	B, X_4	Breaking Stress (GPa)	Initial Modulus (GPa)	Birefringence ($\times 10^{-3}$)
1	−1	−1	−1	−1	0.72	5.4	31
2	1	−1	−1	−1	0.69	5.0	30
3	−1	1	−1	−1	0.74	6.5	32
4	1	1	−1	−1	0.73	5.6	31
5	−1	−1	1	−1	0.73	6.3	32
6	1	−1	1	−1	0.73	5.9	32
7	−1	1	1	−1	0.75	6.7	33
8	1	1	1	−1	0.76[a]	6.8	34
9	−1	−1	−1	1	0.66	4.4	29
10	1	−1	−1	1	0.63	4.3	30
11	−1	1	−1	1	0.69	5.6	32
12	1	1	−1	1	0.68	5.2	32
13	−1	−1	1	1	0.67	6.0	31
14	1	−1	1	1	0.65	5.9	30
15	−1	1	1	1	0.70	6.4	33
16	1	1	1	1	0.69	6.3	32
17	−2	0	0	0	0.67	6.7	32
18	2	0	0	0	0.67	6.8	33
19	0	−2	0	0	0.68	6.4	32
20	0	2	0	0	0.75	6.9	33
21	0	0	−2	0	0.67	5.4	30
22	0	0	2	0	0.74	7.5	32
23	0	0	0	−2	0.65	5.2	32
24	0	0	0	2	0.67	4.8	31
25	0	0	0	0	0.75	7.0	34
26	0	0	0	0	0.76	7.3	35
27	0	0	0	0	0.75	6.6	34
28	0	0	0	0	0.74	7.3	34
29	0	0	0	0	0.76	7.2	35
30	0	0	0	0	0.74	6.8	34
31	0	0	0	0	0.75	6.7	34

[a] Assumed value of sample 8 instead of 0.85 GPa.

Table IV Optimum Parameters for Breaking Stress and Modulus

Variables	Breaking Stress	Initial Modulus
X_1 First zone temp T_1 (°C)	55	54
X_2 First zone draw ratio λ_1	2.55	2.42
X_3 Second zone temp T_2 (°C)	126	131
X_4 HMPP blend composition (%)	4.8	5.7
F (model)[a]	5.60	9.86
R^2	0.83	0.90
Standard error of estimate	0.012	0.16

[a] $F_{10,6,0.95} = 4.06$ (table).

each are given in Table II and investigated by the statistical central composite second order rotatable design.[20] The effect of variables were evaluated at five levels selected on the basis of our previous work.[2,3] The drawing in second zone was carried out to the maximum possible draw ratio. The total draw ratio for all set of samples was in the range of 7 × to 8 ×. The general form of quadratic equation is

$$y = b_0 + b_1X_1 + b_2X_2 + b_3X_3 + b_4X_4 + b_{11}X_1^2 + b_{22}X_2^2 + b_{33}X_3^2 + b_{44}X_4^2 + b_{12}(X_1X_2) + b_{13}(X_1X_3) + b_{14}(X_1X_4) + b_{23}(X_2X_3) + b_{24}(X_2X_4) + b_{34}(X_3X_4)$$

where X subscripts correspond to the numbers given above for independent variables and y denotes the measured response variables. Center point and unit value for the five predictor variables is given in Table III. To test the estimated regression equation for the goodness to fit, the F-test was employed and the coefficient of determination and standard error of estimates were also determined. The second-order polynomial derived from the experimental data was converted into a canonical equation to get the stationary points (Table IV). Contour diagrams were plotted to study the effect of variables on the measured responses. All the analyses were done with the help of an ICL 2960 computer.

REFERENCES

1. G. Hinrichsen and W. Green, *Hunststoffe*, **71**, 2 (1981).
2. B. L. Deopura and S. Kadam, *J. Appl. Polym. Sci.*, **31**, 2145 (1986).
3. D. G. Bet, V. K. Srivastava, B. P. Mani, and B. L. Deopura, 43rd All India Conference, The Textile Association India, Bombay, December 15–16, 1986, p. 276.
4. R. P. Runt, *Encyclopedia of Polymer Science and Engineering*, 2nd ed., Mark, Atlas, Bikalis, Overburger, Menges, Eds., John Wiley & Sons, New York, 1986, Vol. 4, p. 482.
5. G. Farrow and D. Preston, *Br. J. Appl. Phys.*, **11**, 353 (1960).
6. Z. W. Wilchinsky, *J. Appl. Phys.*, **30**, 792 (1959); **31**, 1969 (1960).
7. R. S. Stein and F. H. Norris, *J. Polym. Sci., Polym. Phys. Ed.*, **21**, 381 (1961).
8. Y. Yamamoto, M. Dewasawa, and S. Kinoshita, *Sen-i Gakkaishi*, **38**, T-10 (1982).
9. M. Takayanagi, K. Imada, and T. Kajiyama, *J. Polym. Sci.*, **C-15**, 75 (1966).
10. M. Takayanagi, M. Kamezawa, and K. Yamada, *J. Appl. Polym. Sci.*, **24**, 1227 (1979).
11. H. Sobue and Y. Tabata, *J. Polym. Sci.*, **39**, 427 (1959).
12. P. G. Anderson and S. H. Carr, *J. Mater. Sci.*, **10**, 870 (1975).
13. A. J. Lovinger and M. L. Williams, *J. Appl. Polym. Sci.*, **25**, 1703 (1980).
14. L. S. Remaly and J. M. Schultz, *J. Appl. Polym. Sci.*, **1**, 114 (1970).
15. L. W. Kleiner, M. R. Radioff, J. M. Schultz, and T. W. Chou, *J. Polym. Sci., Polym. Phys. Ed.*, **12**, 819 (1974).
16. N. Morosoff, K. Sakaoku, and A. Peterlin, *J. Polym. Sci. A-2*, **10**, 1221 (1972).
17. F. J. Balta-Calleja, and A. Peterlin, *Macromol. Chem.*, **141**, 91 (1971).
18. H. Tanaka and F. Korogi, *Eur. Polym. J.*, **24**, 759 (1988).
19. C. Jourdan, J. Y. Cavaille, and J. Perez, *J. Polym. Sci., Polym. Phys. Ed.*, **27**, 2361 (1989).
20. G. E. P. Box and J. S. Hunter, *Ann. Math. Stat.*, **28**, 195 (1957).

Received June 20, 1990
Accepted November 9, 1990